Redox-Switched Bonding of Protons to Ferrocenophanes, Ferrocene Cryptands, and Simple Ferrocene Amines. Correlation of X-ray Structural Data and Cyclic Voltammetry Derived Redox Potentials

Herbert Plenio,*,† Jianjun Yang,‡ Ralph Diodone,† and Jürgen Heinze‡

Institut für Anorganische und Analytische Chemie and Institut für Physikalische Chemie, Universität Freiburg, Albertstr. 21, 79104 Freiburg, Germany

Received February 9, 1994®

To gain a better understanding of the redox-switched bonding of cations to ferrocene crown ethers, the redox potentials of 22 ferrocene nitrogen compounds, including protonated and methylated congeners, were determined. The redox potentials of the ammonium salts are shifted by between +110 and +600 mV relative to those of the neutral ferrocenes. Methylation consistently gives slightly larger positive shifts than protonation. The syntheses and X-ray crystal structures of diprotonated [1,1′-ferrocenediylbis(methylene)]bis(*N*-7-aza-2,3-benzo-1,4-dioxacyclononane) (orthorhombic, *Pbca*; a = 11.492(2) Å, b = 16.034(3) Å, c = 18.030(4) Å; V = 3322.3(11) Å^3; R indices [$4(\sigma)I$] R_1 = 4.39%, wR_2 = 11.5%), methylated *N*-methyl-2-aza-[3]-1,1′-ferrocenophane (monoclinic $P2_1/c$; a = 8.396(2) Å, b = 12.336(2) Å, c = 13.414(3) Å, β = 95.16(3)°, V = 1383.7(5) Å^3; R indices [$4(\sigma)I$] R_1 = 2.86%, wR_2 = 7.53%), and dimethylated 7,16-(1,1′-ferrocenediylbis(methylene))-1,4,10,13-tetraoxa-7,16-diazacyclooctadecane (triclinic $P\bar{1}$; a = 10.522(2) Å, b = 12.664(3) Å, c = 13.374(3) Å, α = 82.25(3)°, β = 76.33(3)°, γ = 78.82(3)°; V = 1691.3(6) Å^3; R indices [$4(\sigma)I$] R_1 = 5.19%, wR_2 = 15.4%) are described. The solid state structural data and the cyclic voltammetry derived redox potentials illustrate a linear relationship ($y = (-2.7 + 2.1x) \times 10^2$) between the inverse iron–nitrogen separation (x) and the shifts of the redox potentials (y) and allow the unambiguous assignment of the structures of the protonated isomers of 7,16-(1,1′-ferrocenediylbis(methylene))-1,4,10,13-tetraoxa-7,16-diazacyclooctadecane.

Introduction

Proton and electron transfer processes constitute the most basic chemical reactions and are of fundamental importance in chemistry, biology, and physics.[1] Cytochrome *c* oxidase is a redox-driven proton pump, translocating one vectorial proton per electron from the matrix to the cytosol of the mitochondrial membranes.[2] The utility of crown ethers for the membrane transport of cations has been demonstrated.[3] However, to give this transport a direction in space a switching mechanism is required, which activates or deactivates the bonding of the substrate once the target area has been reached.[4]

Two classes of redox-switched crown ethers are known.[5] Anthraquinone-linked crown ethers show increased bonding of cations upon reduction;[6,7] ferrocene crown ethers on the other hand display a sharp drop in the complex stability upon oxidation.[5] A switching effect occurs as the oxidation of the ferrocene subcomponent generates a positive charge. The proximity of this positively charged group to the crown ether bound cation leads to a destabilization of the whole complex and ideally to a dissociation of the crown ether cation complex. The switching effect is based on the ready reversibility of the oxidation of the ferrocene unit[8] and hence the restoration of the ability to bind cations. The effects, however, which determine the extent of the switching operation have not been fully understood. As part of our activities in the development of molecular switches,[9] we recently described the redox-switched bonding of alkaline metal cations and protons to ferrocene bis(crown ethers) and ferrocene cryptands.[10]

To gain a better understanding into the factors which determine the extent of this redox-switched bonding in ferrocene macrocycles, we investigated more closely the effect of the protonation of nitrogen on the redox potentials of a number of ferrocene nitrogen compounds.

For this purpose we carried out X-ray crystal structure determinations and cyclic voltammetry measurements with the aim of establishing a correlation between the Fe–N distances and the positive shifts of the redox potentials of ferrocene crown ethers, ferrocene cryptands, ferrocenophanes, simple ferrocene amines, and their protonated or methylated cationic derivatives.

Experimental Section

All reactions were carried out under dry nitrogen using standard Schlenk techniques. Commercially available solvents and reagents were purified

† Institüt für Anorganische und Analytische Chemie, Universität Freiburg.
‡ Institüt für Physikalische Chemie, Universität Freiburg.
® Abstract published in *Advance ACS Abstracts,* July 15, 1994.

(1) (a) *Electron Transfer in Biology and the Solid State*; Johnson, M. K., King, R. B., Kurtz, D. M., Kutal, C., Norton, M. L., Scott, R. A., Eds.; ACS Symposium Series 226, American Chemical Society: Washington, DC, 1990. (b) *Electron Transfer in Inorganic, Organic and Biological Systems*, Bolton, J. R., Matagoi, N., McLendon, G., Eds.; ACS Symp. Ser. 228, American Chemical Society: Washington, DC, 1991. (c) Bell, R. P. *The Proton in Chemistry*, 2nd ed.; Cornell University Press: Ithaca, NY, 1973.
(2) Malmström, B. G. *Acc. Chem. Res.* **1993**, *26*, 332.
(3) (a) Saji, T.; Kinoshita, I. *J. Chem. Soc., Chem. Commun.* **1986**, 716. (b) Li, Y.; Gokel, G. W.; Hernandez, J.; Echegoyen, L. *J. Am. Chem. Soc.* **1994**, *116*, 3087.
(4) DeSantis, G.; Fabrizzi, L.; Licchelli, M.; Pallavicini, P. In *Crown Ether Compounds*; Cooper, S. R., Ed.; VCH: Weinheim, Germany, 1992; Chapter 9.
(5) (a) Beer, P. D. *Adv. Inorg. Chem.* **1992**, *39*, 79. (b) Beer, P. D.; Danks, J. P.; Hesek, D.; McAleer, J. F. *J. Chem. Soc., Chem. Commun.* **1993**, 2107. (c) Beer, P. D.; Crowe, D. B.; Ogden, M. I.; Drew, M. G. B.; Main, B. *J. Chem. Soc., Dalton Trans.* **1993**, 2107. (d) Lowe, N. D.; Garner, C. D. *J. Chem. Soc., Dalton Trans.* **1993**, 3333. (e) Hall, C. D.; Tucker, J. H. R.; Chu, S. Y. F.; Parkins, A. W.; Nyborg, S. C. *J. Chem. Soc., Chem. Commun.* **1993**, 1505.
(6) Echegoyen, L.; Hafez, Y.; Lawson, R. C.; deMendoza, J.; Torres, T. *J. Org. Chem.* **1993**, *58*, 2009.
(7) Miller, S. R.; Gustowski, D. A.; Chen, Z.; Gokel, G. W.; Echegoyen, L.; Kaifer, A. E. *Anal. Chem.* **1988**, *60*, 2021.
(8) Geiger, W. E. In *Organometallic Radical Processes*; Trogler, W. C., Ed.; Elsevier: Amsterdam, 1990; p 142.
(9) (a) Goulle, V.; Harriman, A.; Lehn, J. M. *J. Chem. Soc., Chem. Commun.* **1993**, 1034. (b) Jorgensen, M.; Lerstrup, K.; Frederiksen, P.; Björnholm, T.; Sommer-Larsen, P.; Schauberg, K.; Brunfeldt, K.; Beechgaard, K. *J. Org. Chem.* **1993**, *58*, 2785. (c) Gilat, S. L.; Kawai, S. H.; Lehn, J. M. *J. Chem. Soc., Chem. Commun.* **1993**, 1439.
(10) Plenio, H.; El-Desoky, H.; Heinze, J. *Chem. Ber.* **1993**, *126*, 2403.

0020-1669/94/1333-4098$04.50/0

according to literature procedures. Chromatography was carried out with silica MN 60. NMR spectra were recorded at 300 K with a Bruker AC200 F (^{1}H NMR 200 MHz, ^{13}C NMR 50 MHz). ^{1}H NMR was referenced to residual hydrogen in the solvent and ^{13}C NMR to the signals of the $CDCl_3$ (7.26 ppm, 77.0 ppm), CD_3CN (1.93 ppm, 1.30 ppm) or DMSO-d_6 solvent (2.49 ppm, 39.5 ppm). Elemental analyses were performed at the Mikroanalytisches Laboratorium der Chemischen Laboratorien, Universität Freiburg. Melting points were determined with a Meltemp melting point apparatus in sealed capillaries. Starting materials were commercially available or prepared according to literature procedures: [1,1′-ferrocenediylbis(methylene)]bis(pyridinium) tosylate chloride,[11] 1-ferrocenyl-2-(dimethylamino)ethane,[12] ferrocenyl (dimethylamino)methane,[13] 7-aza-2,3-benzo-1,4-dioxacyclononane,[14] 7,16-(1,1′-ferrocenediylbis(methylene))-1,4,10,13-tetraoxa-7,16-diazacyclooctadecane,[10] *N*-methyl-3,4-ferrocenediyl-1-aza-cyclohexane.[15]

Cyclic Voltammetry. The standard electrochemical instrumentation consisted of a PAR Model 173 potentiostat/galvanostat and a PAR Model 175 universal programmer. Cyclic voltammograms were recorded with a Philips Model PM 8033 X-Y recorder. A three-electrode configuration was employed. The working electrode was a Pt disk (diameter 1 mm) sealed in soft glass. The counter electrode was a Pt wire coiled around the glass mantle of the working electrode. The reference electrode was an Ag wire on which AgCl had been deposited electrochemically. Potentials were calibrated against the formal potential of cobaltocenium perchlorate (–0.94 V vs Ag/AgCl). All measurements were carried out in CH_3CN under strictly anhydrous conditions with NBu_4PF_6 as supporting electrolyte.

1-Ferrocenyl-2-(dimethylamino)ethane (2). Preparation was as described in ref 12. ^{1}H NMR ($CDCl_3$): δ 2.27 (s, 6H, $N(CH_3)_2$), 2.45–2.49 (m, 4H, CH_2CH_2), 4.04–4.08 (m, 4H, FcH), 4.11 (s, 5H, FcH). ^{13}C NMR ($CDCl_3$): δ 27.90 (CH_2N), 45.50 (CH_3), 60.93 ($FcCH_2$), 67.16 (FcH), 68.07 (FcH), 68.47 (FcH), 86.76 (Fc).

(Ferrocenylmethylene)trimethylammonium Tetrafluoroborate (3b). Equimolar amounts of $Me_3O^+BF_4^-$ and $FcCH_2NMe_2$ were stirred in acetonitrile for 2 h. The volatiles were removed in vacuo, and the residue was recrystallized from CH_3CN/Et_2O. Anal. Calcd for $C_{14}H_{20}BF_4FeN$ (*M* 344.98): C, 48.74; H, 5.84; N, 4.06. Found: C, 48.43; H, 5.78; N, 4.36. ^{1}H NMR (DMSO-d_6): δ 2.88 (s, 9H, CH_3), 4.23 (s, 5H, FcH), 4.30 (s, 2H, $FcCH_2$), 4.37 ("t", *J* = 1.8 Hz, 2H, FcH), 4.45 ("t", *J* = 1.8 Hz, 2H, FcH). ^{13}C NMR (DMSO-d_6): δ 52.88 (t, J_{NC} = 4 Hz, CH_3), 67.85 (t, J_{NC} = 2.4 Hz, $FcCH_2$), 70.21 (FcH), 71.46 (FcH), 73.12 (FcH), 73.55 (Fc).

[1,1′-Ferrocenediylbis(methylene)]bis(dimethylamine) (4). To a solution of Me_2NH (1.13 g, 25 mmol) in 30 mL of CH_3CN was added [1,1′-ferrocenediylbis(methylene)]bis(pyridinium) tosylate chloride (1.3 g, 2.3 mmol) and the reaction mixture heated under reflux for 14 h. Silica was added to the cold solution and the volatiles removed in vacuo. The residue was poured on top of a 5-cm layer of silica and the product extracted with cyclohexane/ethyl acetate (1:1). The solvent was removed in vacuo and the product remains as a red oil. Yield: 0.45 g (65%). Anal. Calcd for $C_{16}H_{24}FeN_2$ (*M* 300.2): C, 64.01; H, 8.06; N, 9.33. Found: C, 64.31; H, 8.24; N, 9.19. ^{1}H NMR ($CDCl_3$): δ 2.15 (s, 12H, CH_3), 3.25 (s, 4H, CH_2), 4.05–4.08 (m, 8H, FcH). ^{13}C NMR ($CDCl_3$): δ 44.70 (CH_3), 58.96 ($FcCH_2$), 68.62 (FcH), 70.59 (FcH), 83.4 (br, Fc).

[1,1′-Ferrocenediylbis(methylene)]bis(trimethylammonium) Tetrafluoroborate (4b). Preparation was analogous to that of $FcCH_2NMe_3BF_4$. Anal. Calcd for $C_{18}H_{30}B_2F_8FeN_2$ (*M* 503.92): C 42.90; H, 6.00; N, 5.56. Found: C, 43.07; H, 5.90; N, 5.70. ^{1}H NMR (DMSO-d_6): δ 2.91 (s, 18 H, CH_3), 4.33 (s, 4 H, $FcCH_2$), 4.46 ("t", *J* = 1.9 Hz, 4H, FcH), 4.50 ("t", *J* = 1.9 Hz, 4H, FcH). ^{13}C NMR (DMSO-d_6): δ 53.01 (t, J_{NC} = 4 Hz, CH_3), 67.05 (t, J_{NC} = 2.4 Hz, CH_2), 72.67 (FcH), 74.43 (FcH), 74.98 (Fc).

[1,1′-Ferrocenediylbis(methylene)]bis(7-aza-2,3-benzo-1,4-dioxacyclononane) (5). A mixture of [1,1′-ferrocenediylbis(methylene)]bis(pyridinium) tosylate chloride (1.15 g, 2 mmol), 7-aza-2,3-benzo-1,4-dioxacyclononane (0.36 g, 2 mmol) and Na_2CO_3 (1.15 g) in CH_3CN was heated to reflux for 36 h. After filtration the volatiles were removed in vacuo. To the residue was added 10 mL of water and the product extracted two times with 50 mL of CH_2Cl_2. The combined organic layers were separated, dried over $MgSO_4$, and filtered, and the CH_2Cl_2 was evaporated. The residue was purified chromatographically (cyclohexane/ethyl acetate/diethylamine). Yield: 0.75 g (66%) of a yellow powder, mp 98 °C. Anal. Calcd for $C_{32}H_{36}FeN_2O_4$ (*M* 568.50): C, 67.61; H, 6.38; N, 4.93. Found: C, 67.71; H, 6.54; N, 5.12. ^{1}H NMR ($CDCl_3$): δ 2.85 (t, *J* = 4.6 Hz, 8H, NCH_2), 3.48 (s, 4H, $FcCH_2$), 3.89 ("t", *J* = 1.7 Hz, 4 H, FcH), 3.97 ("t", *J* = 1.7 Hz, 4H, FcH), 4.20 (t, *J* = 4.6 Hz, 4H, OCH_2), 6.91 (s, 8H, ArH). ^{13}C NMR ($CDCl_3$): δ 55.40 (CN), 56.97 (CN), 68.49 (CH_2O), 70.27 (FcH), 73.38 (FcH), 83.92 (Fc), 122.49 (ArH), 123.39 (ArH), 151.53 (ArO).

5·2HClO$_4$ (5a). **5** (57 mg, 0.1 mmol) and $HClO_4$ (70% in H_2O, 0.3 mmol) were mixed in Et_2O. A yellow precipitate formed immediately and was filtered off after 1 h of stirring. The yellow solid was dried in vacuo and recrystallized from CH_3CN/Et_2O. Anal. Calcd for $C_{32}H_{38}Cl_2FeN_2O_{12}$ (*M* 769.42): C, 49.95; H, 4.98; N, 3.64. Found: C, 49.83; H, 4.90; N, 3.74. ^{1}H NMR (CD_3CN): δ 3.50 (t, *J* = 5.2 Hz, 8H, NCH_2), 4.27 (t, *J* = 5.1 Hz, 8H, OCH_2), 4.43 (s, 4H, $FcCH_2$), 4.47 ("t", *J* = 1.9 Hz, 4H, FcH), 4.61 ("t", *J* = 1.9 Hz, 4H, FcH), 7.12 (s, 8H, ArH). ^{13}C NMR (CD_3CN): δ 54.23 (NC), 58.53 (NC), 69.96 (CH_2O), 72.57 (FcH), 73.65 (FcH), 76.19 (Fc), 124.24 (ArH), 127.00 (ArH), 151.64 (ArO).

N-Methyl-2-aza-[3]-1,1′-ferrocenophane (6). A suspension of **1** (1.15 g, 2 mmol), Na_2CO_3 (1.15 g) in 50 mL of CH_3CN was heated under reflux, a solution of $MeNH_2$ (0.15 g, 2.5 mmol) in 40 mL of CH_3CN slowly added dropwise and heating continued for 12 h. Yield: 35% of yellow powder, mp 116 °C. Anal. Calcd for $C_{13}H_{15}FeN$ (*M* 241.1): C, 64.76; H, 6.27; N, 5.81. Found: C, 64.63; H, 6.23; N, 5.85. ^{1}H NMR ($CDCl_3$): δ 2.55 (s, 3H, CH_3), 2.80 (s, 4H, CH_2), 4.09 (s, 8H, FcH). ^{13}C NMR ($CDCl_3$): δ 46.22 (NCH_3), 54.41 (NCH_2), 69.25 (FcH), 69.85 (FcH), 83.44 (Fc).

2-N,N-Dimethylammonium-[3]-1,1′-ferrocenophane Tetrafluoroborate (6b). Preparation was analogous to that of $FcCH_2NMe_3BF_4$. Anal. Calcd for $C_{14}H_{18}BF_4FeN$ (*M* 342.96): C, 49.03; H, 5.29; N, 4.08. Found: C, 49.40; H, 5.26; N, 4.24. ^{1}H NMR (DMSO-d_6): δ 3.28 (s, 6H, CH_3), 3.78 (s, 4H, CH_2), 4.30 ("t", *J* = 1.9 Hz, 4 H, FcH), 4.37 ("t", 4 H, *J* = 1.9 Hz, FcH). ^{13}C NMR (DMSO-d_6): δ 53.79 (t, J_{NC} = 4 Hz, CN), 60.48 (br, CN), 72.71 (FcH), 73.18 (FcH), 74.77 (Fc).

2-N,N-Dimethylammonium-[3]-1,1′-ferrocenophane Iodide (6c). (0.63 g, 2.2 mmol) of **6** was suspended in 15 mL of CH_3CN and CH_3I (0.625 g, 4.4 mmol) added, whereupon a clear solution rapidly formed. After 1 h the product precipitated and was filtered off. The yellow solid was dried in vacuo and recrystallized from CH_3CN/Et_2O. Yield: 0.8 g (95%) of a yellow powder. Anal. Calcd for $C_{14}H_{18}FeIN$ (*M* 383.05): C, 43.72; H, 4.63; N, 3.81. Found: C, 43.90; H, 4.74; N, 3.66. ^{1}H NMR (DMSO-d_6): δ 3.32 (s, 6H, CH_3), 3.95 (s, 4H, CH_2), 4.36 (s, 8H, FcH). ^{13}C NMR (DMSO-d_6): δ 52.19, 57.84, 71.30 (FcH), 71.96 (FcH), 74.40 (Fc).

***N*-Methyl-3,4-ferrocenediyl-1-azacyclohexane (7).** Preparation was as described in ref 15. ^{1}H NMR ($CDCl_3$): δ 2.42 (s, 3H, CH_3), 2.51–2.62 (m, 2H, CH_2CH_2), 2.68–2.80 (m, 2H, CH_2CH_2), 3.36 (d, *J* = 13.6 Hz, 1H, C*H*H), 3.48 (d, *J* = 13.5 Hz, 1H, CH*H*), 3.95 (t, *J* = 2.3 Hz, 1H, FcH), 4.04 (s, 7H, FcH). ^{13}C NMR ($CDCl_3$): δ 25.34 ($FcCH_2$), 45.99 (CN), 52.92 (CN), 55.04 (CN), 63.44 (FcH), 64.49 (FcH), 65.22 (FcH), 69.58 (FcH), 83.18 (Fc), 83.46 (Fc).

7,16-(1,1′-Ferrocenediylbis(methylene))-1,4,10,13-tetraoxa-7,16-diazacyclooctadecane–Bis(methyl iodide) (8c). Preparation was analogous to that of **4c**. Anal. Calcd for $C_{26}H_{42}FeI_2N_2O_4$ (*M* = 756.28): C, 41.29; H, 5.60; N, 3.70. Found: C, 41.77; H, 5.48; N, 3.79. ^{1}H NMR (CD_3CN): δ 2.92 (s, 6H, CH_3), 3.29 and 3.36 (t, *J* = 3.5 Hz, 4H), 3.52–3.68 (m, 8H), 3.81–3.94 (m, 12H), 4.46 ("t", 4 H, FcH), 4.51 (s, 4H, $FcCH_2$), 4.70 ("t", 4H, FcH). ^{13}C NMR (CD_3CN): δ 51.13, 61.26, 63.68, 65.02, 70.69, 72.84, 74.05, 75.91, 89.04.

Crystallographic Data Collection

Crystals of **5a**, **6c**, and **8c** were grown from CH_3CN/Et_2O and mounted on top of a glass fiber. X-ray data were collected on an Enraf-Nonius CAD4 diffractometer with Mo Kα radiation (71.069 pm) and a graphite monochromator. Structure solution and structure refinement on F^2 used SHELXS 86[16] and SHELXL 93,[17] respectively.

Crystal Structure Determination of 5a. Crystal dimensions: 0.5 × 0.5 × 0.4 mm^3. θ range: 2.3–28.4°. Index range (*hkl*:

(11) Tverdokhlebov, V. P.; Tselinskii, I. V.; Gidaspov, B. V.; Chikisheva, G. Y. *J. Org. Chem. USSR* (*Engl. Transl.*) **1976**, *12*, 2268.
(12) Hauser, C. R.; Lindsay, J. K.; Lednicer, D. *J. Org. Chem.* **1958**, *23*, 358.
(13) Goldberg, S. I.; Bailey, W. D. *J. Am. Chem. Soc.* **1974**, *96*, 6381.
(14) Högberg, S. A. G.; Cram, D. J. *J. Org. Chem.* **1975**, *40*, 151.
(15) Lednicer, D.; Lindsay, J. K.; Hauser, C. R. *J. Org. Chem.* **1958**, *23*, 653.
(16) Sheldrick, G. M. SHELXS 86. Universität Göttingen, 1990.
(17) Sheldrick, G. M. SHELXL 93. Universität Göttingen, 1993.

−15, 0; (0, 20); −23.0. Space group: orthorhombic *Pbca*. $F(000)$ = 1600. Absorption correction: empirical, ψ scans. $T_{min/max}$ = 0.75/0.96. Refinement method: full-matrix least squares on F^2. Reflections (collected, independent): 3706, 3706. Data/parameter = 3196/226. GooF = 1.017. Weights: w_1 = 0.0619; w_2 = 3.60. Largest difference peak and hole = +0.693 and −0.381 e/Å^3, respectively. All non-hydrogen atoms were refined with anisotropic thermal parameters. All hydrogen atoms were refined with fixed isotropic temperature coefficients (riding model), except for the ammonium hydrogen which was localized and refined independently.

Crystal Structure Determination of 6c. Crystal dimensions: 0.3 × 0.3 × 0.3 mm^3. θ range: 2.5–33°. Index range: (*hkl*): −12, 12; −18, 0; 0, 20. Space group: monoclinic $P2_1/c$. $F(000)$ = 752. Absorption correction: empirical, ψ scans. $T_{min/max}$ = 0.66/0.88. Refinement method: full-matrix least squares on F^2. Reflections (collected, independent): 5401, 5217. Data/parameter = 4852/155. GooF: 1.098. Weights: w_1 = 0.0364; w_2 = 0.97. Largest difference peak and hole = +1.07, −1.01 e/Å^3. All non-hydrogen atoms were refined with anisotropic thermal parameters. All hydrogen atoms were refined with fixed isotropic temperature coefficients (riding model).

Crystal Structure Determination of 8c. Crystal dimensions: 0.7 × 0.5 × 0.2 mm^3. θ range: 2.8–26°. Index range (*hkl*): −12, 12; −15, 0; −16, 16. Space group: triclinic, $P\bar{1}$. $F(000)$ = 752. Density: 1.485 g cm^{-3}. Absorption coefficient: 2.299 mm^{-1}. Absorption correction: empirical, ψ scans. $T_{min/max}$ = 0.58/1.00. Refinement method: full-matrix least squares on F^2. Reflections (collected, independent): 6870, 6569. Data/parameter = 6026/352. GooF = 1.10. Weights: w_1 = 0.102; w_2 = 2.33. Largest difference peak and hole = +1.31, −0.95 e/Å^3. The crystal of **8c** contains two solvent molecules (CH_3CN and H_2O) which were included in the refinement with partial site occupancy factors. All non-hydrogen atoms were refined with anisotropic thermal parameters. All hydrogen atoms were refined with fixed isotropic temperature coefficients (riding model). GooF and weight are defined as follows: $\text{GooF} = \sigma[w(F_o^2 - F_c^2)^2/(n-p)^{0.5}$; $w = [\sigma^2(F_o^2) + (w_1{*}P)^2 + w_2{*}P]^{-1}$.

Results and Discussion

It has been suggested that four factors are mainly responsible for the redox-switching effect in electrochemically-active crown ethers: charge density of the bound cation, iron–positive charge distance, mesomeric interaction of the crown ether bound cation with the ferrocene, and, to a lesser extent, cation binding strength.[5] To determine the contribution of a single one of these factors to the overall effect, all but one variable should be held constant. For a given metal cation the charge density has a fixed value, but it is not obvious how either the binding strength or the distance iron–positive charge are to be held constant within a series of ferrocene cryptands or ferrocene crown ethers. For H^+, however, the situation is less complicated. The proton is not symmetrically bound within the cavity of azaoxa macrocycles but rather only to a single nitrogen lone pair,[18] as the basicity of amines by far exceeds that of the ether oxygen. Also it is easy to maintain a fairly constant proton binding strength if the only basic centers are tertiary amines. Ideally, this cation binding strength (or basicity) of the ligands will be high enough to bind the majority of the cations in the reduced state and release most upon oxidation.

The simple ferrocene amines **2**, **3**, **4**, and **7** have already been described in the literature[12,13,15] (Figure 1). However, the reaction of excess bis(dimethylamino)methane with ferrocene only gives a small yield of **4**.[19] We have improved the synthesis of **4** which can now be obtained in 66% yield upon treatment of [1,1′-ferrocenediylbis(methylene)]bis(pyridinium) tosylate chloride (**1**)

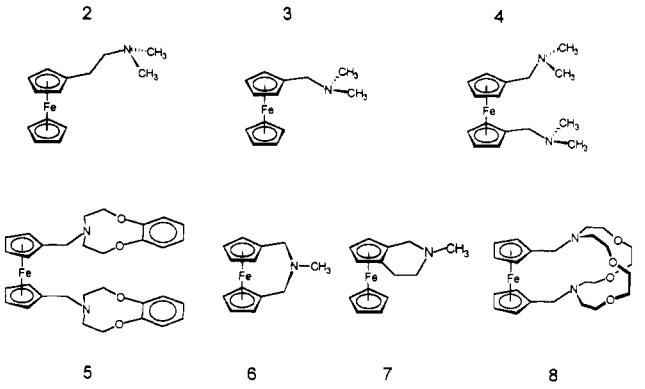

Figure 1. Ferrocene–nitrogen compounds.

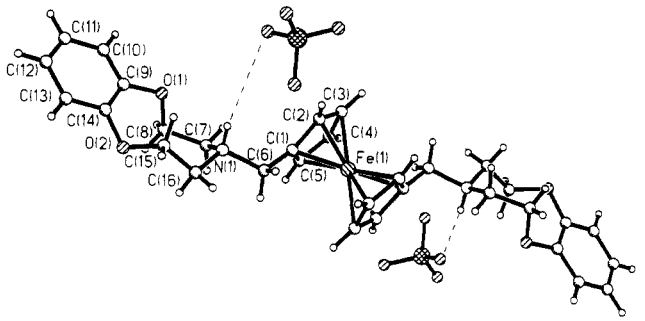

Figure 2. Molecular structure of **5a**.

with an excess of dimethylamine. The bis(crown ether) **5**, which is closely related to **4**, was synthesized in the reaction of **1** and 7-aza-2,3-dibenzo-1,3-dioxacyclononane with the same yield as **4**. The ferrocenes **2–4** are alkylated by CH_3I or $(CH_3)_3O^+BF_4^-$ in almost quantitative yields.

The amines **2–5** are characterized by a flexible geometry of the sidechain, resulting in a maximum iron–nitrogen distance once the protonated or methylated ferrocene amine is oxidized. Much larger positive shifts of the redox potential upon protonation can be expected for a rigid geometry and a small Fe–N distance. We set out to therefore synthesize a ferrocenophane which has a nitrogen atom in a short chain bridging the two rings. Thereby a small and fixed iron–nitrogen distance is forced onto the rigid molecule. The reaction of **1** with methylamine in a 1:1 ratio gives the novel *N*-methyl-2-aza-[3]-ferrocenophane (**6**) in a 30% yield. The asymmetric nature of the three-atom bridge between the two cyclopentadienyl rings generates two isomers which differ with respect to the orientation of the nitrogen methyl group. However, the rapid inversion of the nitrogen equilibrates the two isomers. Alkylation of **6** with $(CH_3)_3O^+BF_4^-$ or CH_3I leads in excellent yield to the corresponding methylated phanes **6b** and **6c**, which also have two chemically inequivalent methyl groups. However, after the quaternization of nitrogen a different isomerization process must be operative, as the 200-MHz ^{1}H-NMR (T = −30 °C) spectra of **6b** and **6c** show equivalent methyl groups on the NMR time scale. The activation barrier for the isomerization processes of ferrocenophanes is often below 50 kJ/mol and is therefore accessible by DNMR only under favorable circumstances.[20] The isomerization is usually viewed as a flipping process of the bridge with an intermediate planarization of the three bridge atoms. However, after recent calculations a transition state involving a staggered orientation of the cyclopentadienyl rings appears more likely.[21]

Solid-State Structures of 5a, 6c, and 8c

In the crystal structure of **5a** the iron atom is situated on a crystallographic center of inversion (Figure 2; Tables 1 and 2). The conformer adopted in the solid state is characterized by a torsion angle C(2)–C(1)–C(6)–N(1) of 90°, resulting in the

(18) Brügge, H. J.; Carboo, D.; vonDeuten, K.; Knöchel, A.; Kopf, J.; Dreissig, W. *J. Am. Chem. Soc.* **1986**, *108*, 107.
(19) Pauson, P. L.; Sandhu, M. A.; Watts, W. F. *J. Chem. Soc. C* **1966**, 251.

Table 1. Atomic Coordinates (×10⁴) for 5a

	x	y	z
Fe(1)	0	5000	0
C(1)	−333(2)	4494(2)	1010(1)
C(2)	−1184(2)	5117(2)	836(2)
C(3)	−1754(3)	4873(2)	180(2)
C(4)	−1287(3)	4107(2)	−62(2)
C(5)	−404(3)	3870(2)	447(2)
C(6)	524(2)	4536(2)	1625(1)
N(1)	88(2)	4160(1)	2356(1)
C(7)	−338(3)	3281(2)	2244(2)
C(8)	−658(3)	2844(2)	2953(2)
O(1)	−1456(2)	3373(1)	3346(1)
C(9)	−1419(2)	3284(2)	4112(1)
C(10)	−2393(3)	3006(2)	4483(2)
C(11)	−2399(3)	2967(2)	5254(2)
C(12)	−1432(3)	3197(2)	5647(2)
C(13)	−439(3)	3455(2)	5284(2)
C(14)	−427(3)	3497(2)	4513(2)
O(2)	598(2)	3702(1)	4161(1)
C(15)	584(3)	4449(2)	3720(2)
C(16)	1022(2)	4272(2)	2938(2)

Table 2. Selected Bond Lengths (pm) and Angles (deg) for 5a

C(6)–N(1)	153.4(3)	N(1)–C(7)	150.6(3)
N(1)–C(16)	151.2(3)	C(7)–C(8)	150.4(4)
C(8)–O(1)	143.5(3)	O(1)–C(9)	148.8(3)
C(9)–C(10)	137.9(4)	C(10)–C(11)	139.2(4)
C(11)–C(12)	136.8(5)	C(12)–C(13)	137.9(5)
C(13)–C(14)	139.3(4)	C(14)–O(2)	137.7(4)
O(2)–C(15)	143.8(3)	C(15)–C(16)	152.3(4)
cent–cent′	329.8(8)		
C(5)–C(1)–C(6)	126.9(3)	C(2)–C(1)–C(6)	125.8(2)
C(10–C(6)–N(1)	114.1(2)	C(7)–N(1)–C(16)	115.8(2)
C(7)–N(1)–C(6)	111.0(2)	C(16)–N(1)–C(6)	108.5(2)
C(8)–C(7)–N(1)	113.7(2)	O(1)–C(8)–C(7)	107.5(2)
C(9)–O(1)–C(8)	114.3(2)	C(14)–O(2)–C(15)	116.4(2)
O(2)–C(15)–C(16)	110.7(3)	N(1)–C(16)–C(15)	115.4(2)

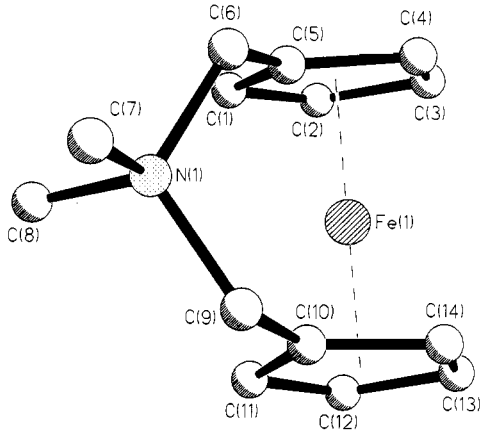

Figure 3. Molecular structure of **6c**.

largest possible Fe–N distance of 456 pm. The NH proton (N–H = 80 pm) is not oriented toward the inside of the nine membered ring and there are no interactions with the oxygen lone pairs. However, there is a weak bridging contact of this hydrogen atom with a perchlorate group over a distance of 213 pm. Bonding parameters within the nine-membered oxaaza ring are in the normal range.

The molecular structure of the cationic ferrocenophane **6c** (Figure 3; Tables 3 and 4) shows a somewhat distorted structure with a 12.2° deviation of the two five-membered rings from coplanarity, whereas the centroid–centroid′ distance of 325.6 pm is not unusual for a ferrocene. The two cyclopentadienyl rings

Table 3. Selected Atomic Coordinates (×10⁴) for 6c

	x	y	z
Fe(1)	2602(1)	6752(1)	4231(1)
C(1)	4673(3)	6969(2)	3573(2)
C(2)	4469(3)	7831(2)	4251(2)
C(3)	3002(4)	8362(2)	3959(2)
C(4)	2283(3)	7823(2)	3100(2)
C(5)	3284(2)	6941(2)	2863(2)
C(6)	2840(3)	6164(2)	2035(2)
N(1)	2616(2)	4976(2)	2307(1)
C(7)	2087(4)	4388(3)	1350(2)
C(8)	4168(3)	4491(2)	2735(2)
C(9)	1308(2)	4776(2)	3019(2)
C(10)	1466(2)	5346(2)	3997(1)
C(11)	2650(2)	5230(2)	4828(2)
C(12)	2297(3)	5994(2)	5574(2)
C(13)	897(3)	6561(2)	5229(2)
C(14)	366(2)	6159(2)	4266(2)

Table 4. Selected Bond Lengths (pm) and Angles (deg) for 6c

C(5)–C(6)	148.9(3)	C(6)–N(1)	152.6(3)
N(1)–C(8)	150.1(3)	N(10–C(7)	150.7(3)
N(1)–C(9)	153.8(3)	C(9)–C(10)	148.5(3)
cent–cent′	325.6(6)		
C(4)–C(5)–C(6)	122.9(2)	C(1)–C(5)–C(6)	130.1(2)
C(5)–C(6)–N(1)	117.8(20	C(8)–N(1)–C(7)	108.3(2)
C(8)–N(1)–C(6)	110.7(2)	C(7)–N(1)–C(6)	106.9(2)
C(6)–N(1)–C(9)	14.4(2)	C(10)–C(9)–N(1)	117.4(2)
C(14)–C(10)–C(9)	123.1(2)	C(11)–C(10)–C(9)	129.9(2)

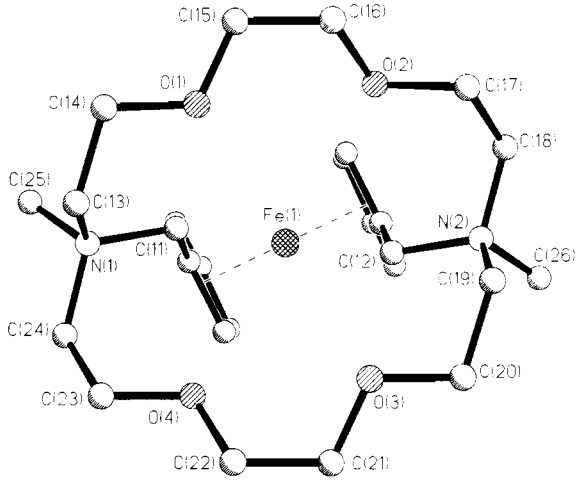

Figure 4. Molecular structure of **8c**.

are virtually planar, the appended carbon atoms C(6) and C(9) being removed from this plane by only 9.9 and 5.7 pm, respectively. These values are well within the range of other ferrocenophanes with a three-atom bridge.[22] The most important feature of this structure is the short Fe–N distance of only 338.5 pm, which is enforced by the rigid geometry of **6c**.

The repulsion of the two positive charges in **8c** leads to a distance of 629 pm between the two cationic nitrogen atoms in the solid-state structure (Figure 4, Tables 5 and 6). However, it is interesting to note that the closest intermolecular nitrogen–nitrogen distance of 705 pm is in the same range. The intramolecular internitrogen distance is almost as large as the 640-pm distance observed in diaza-18-crown-6.[23] Whereas in the structure of **8** the ferrocene clamp leads to an elliptical distortion of the 18-membered ring (N–N = 458 pm),[10] the ring

(20) Herberhold, M.; Brendel, H.-D. *J. Organomet. Chem.* **1993**, *458*, 205.
(21) Abel, E. W.; Orrell, K. G.; Osborne, A. G.; Sik, V.; Guoxiong, W. *J. Organomet. Chem.* **1991**, *411*, 239.
(22) (a) Batail, P.; Grandjean, D.; Astruc, D.; Dabard, R. *J. Organomet. Chem.* **1975**, *102*, 79. (b) Lecomte, C.; Dusausoy, Y.; Protas, J.; Moise, C. *Acta Crystallogr., Sect. B* **1973**, *29*, 1127. (c) Jones, N. D.; March, R. E.; Richards, J. H. *Acta Crystallogr., Sect. B* **1965**, *19*, 330. (d) Lecomte, C.; Dusausoy, Y.; Protas, J. *Acta Crystallogr., Sect. B* **1973**, *29*, 488.
(23) Herceg, M.; Weiss, R. *Bull. Chim. Soc. Fr.* **1972**, 549.

Table 5. Selected Atomic Coordinates (×10⁴) for 8c

	x	y	z
Fe(1)	-3977(1)	122(1)	7323(1)
C(1)	-5730(5)	233(4)	8379(4)
C(2)	-4799(7)	-605(5)	8726(4)
C(3)	-3722(7)	-170(5)	8804(4)
C(4)	-3948(5)	972(5)	8507(4)
C(5)	-5215(5)	1215(4)	8237(3)
C(6)	-4198(5)	424(4)	5834(3)
C(7)	-4015(6)	-713(4)	6126(4)
C(8)	-2797(5)	-1036(4)	6422(4)
C(9)	-2190(5)	-109(4)	6328(4)
C(10)	-3048(4)	799(3)	5944(3)
C(11)	-5813(5)	2281(4)	7769(3)
C(12)	-2834(4)	1943(3)	5815(3)
N(1)	-6804(4)	2984(3)	8559(3)
C(13)	-7330(5)	4042(4)	7989(4)
C(14)	-7878(5)	3925(4)	7082(4)
O(1)	-6837(3)	3922(3)	6183(3)
C(15)	-7140(5)	3537(4)	5336(4)
C(16)	-6041(5)	3645(4)	4411(4)
O(2)	-4884(3)	2921(3)	4569(2)
C(17)	-3801(5)	3009(4)	3719(4)
C(18)	1993(4)	2285(3)	4757(3)
C(19)	-1780(5)	3438(4)	4753(4)
C(20)	-1251(5)	3651(4)	5656(5)
O(3)	-2352(3)	3965(3)	6456(3)
C(21)	-1991(6)	3965(5)	7416(5)
C(22)	-3195(6)	4379(5)	8196(5)
O(4)	-4129(4)	3667(3)	8386(3)
C(23)	-5242(6)	4007(5)	9159(5)
C(24)	-6189(5)	3197(5)	9416(4)
C(25)	-7943(5)	2397(5)	9065(4)
C(26)	-671(4)	1549(4)	4581(4)

Table 6. Selected Bond Lengths (pm) and Angles (deg) for 8c

C(11)-N(1)	153.9(5)	C(12)-N(2)	153.8(5)
N(1)-C(25)	150.8(7)	N(1)-C(24)	151.9(7)
N(1)-C(13)	152.2(7)	C(13)-C(14)	149.7(8)
C(14)-O(1)	142.2(6)	O(1)-C(15)	141.5(6)
C(15)-C(16)	149.2(7)	C(16)-O(2)	141.6(6)
O(2)-C(17)	141.7(6)	C(17)-C(18)	151.2(7)
C(18)-N(2)	149.7(6)	N(2)-C(26)	150.4(5)
N(2)-C(19)	151.8(6)	C(19)-C(20)	151.9(8)
C(20)-O(3)	141.3(6)	O(3)-C(21)	142.2(7)
C(21)-C(22)	149.5(9)	C(22)-O(4)	141.8(7)
O(4)-C(23)	140.7(6)	C(23)-C(24)	151.8(8)
cent-cent′	328.6(9)		
C(10-C(5)-C(11)	126.2(5)	C(4)-C(5)-C(11)	125.9(5)
C(6)-C(10)-C(12)	126.7(4)	C(9)-C(10)-C(12)	125.1(4)
C(5)-C(11)-N(1)	113.8(30	C(10)-C(12)-N(2)	114.2(3)
C(25)-N(1)-C(24)	106.9(4)	C(25)-N(1)-C(13)	109.2(4)
C(24)-N(1)-C(13)	110.7(4)	C(25)-N(1)-C(11)	109.0(4)
C(24)-N(1)-C(11)	112.3(4)	C(13)-N(1)-C(11)	108.6(3)
C(14)-C(13)-N(1)	115.2(4)	O(1)-C(14)-C(13)	108.4(4)
C(15)-O(1)-C(14)	113.0(4)	O(1)-C(15)-C(16)	109.2(4)
O(2)-C(16)-C(15)	109.5(4)	C(16)-O(2)-C(17)	111.7(4)
O(2)-C(17)-C(18)	110.9(4)	N(2)-C(18)-C(17)	117.5(4)
C(18)-N(2)-C(26)	105.8(4)	C(18)-N(2)-C(19)	110.7(4)
C(26)-N(2)-C(19)	109.3(4)	C(18)-N(2)-C(12)	112.9(3)
C(26)-N(2)-C(12)	109.4(3)	C(19)-N(2)-C(12)	108.8(3)
N(2)-C(19)-C(20)	115.3(4)	O(3)-C(20)-C(19)	107.6(4)
C(20)-O(3)-C(21)	112.7(4)	O(3)-C(21)-C(22)	109.1(5)
O(4)-C(22)-C(21)	110.2(4)	C(23)-O(4)-C(22)	111.3(4)
O(4)-C(23)-C(24)	111.1(4)		

in **8c** is almost circular. The 12 carbon and the four oxygen atoms of the macrocycle are approximately coplanar (mean deviation 40 pm), which contrasts with the puckered ring observed in **8**. The mean iron–nitrogen distance of 446 pm is 10 pm shorter than that in **5a**. Half the torsion angles within the macrocycle are 164–179°, the other nine range from 49 to 91°, indicative of some strain within the ring. The geometry of the ferrocene unit is unspectacular. More important is the exo, exo orientation of the two methyl groups with respect to the macrocyclic ring. Whereas the proton is small enough to migrate directly into the cavity to form the endo, endo isomer, this is prevented by the bulk of the CH_3^+ group. Thus methylation of **8** is only possible in the exo, exo orientation of the nitrogen lone pairs.

Table 7. Crystallographic Data for 5a, 6b, and 8c

chem formula	$C_{32}H_{38}Cl_2FeN_2O_{12}$	$C_{14}H_{18}FeIN$	$C_{26}H_{42}FeI_2N_2O_4$
a, Å	11.492(2)	8.396(2)	10.522(2)
b, Å	16.034(3)	12.336(2)	12.664(3)
c, Å	18.030(4)	13.414(3)	13.374(3)
α, deg	90	90	82.258(3)
β, deg	90	95.16(3)	76.33(3)
γ, deg	90	90	78.82(3)
V, Å³	3322.3(11)	1383.7(5)	1691.3(6)
Z	4	4	2
fw	769.39	383.04	756.27
T, K	295	295	295
λ, pm	71.069	71.069	71.069
ρ, g cm⁻³	1.538	1.839	1.485
μ, mm⁻¹	0.682	3.299	2.299
R_1[a]	4.39%	2.86%	5.19%
wR_2[a]	11.5%	7.53%	15.4%

[a] R_1 and wR_2 are defined as follows: $R_1 = \sigma|F_o - F_c|/\sigma(F_o)$; $wR_2 = [\sigma[w(F_o^2 - F_c^2)^2/\sigma[w(F_o^2)^2]]^{0.5}$.

Table 8. Electrochemical Data for the Different Ferrocene–Nitrogen Compounds [*E*(1)] and Their Protonated or Methylated Relatives [*E*(2)][a]

	E(1), V	*E*(2), V	*E*(2) - *E*(1), mV
2/2a	+0.32	+0.43	+110
3/3a	+0.42	+0.60	+185
3b		+0.61	+190
4/4a	+0.38	+0.80	+420
4b		+0.84	+460
5/5a	+0.37	+0.81	+440
6/6a	+0.38	+0.73	+350
6b		+0.77	+390
7/7a	+0.29	+0.52	+230
8/8*H⁺	+0.25	+0.47/+0.60	+220/+350
8*H⁺H⁺		+0.75/+0.85	+500/+600
8c		+0.80	+550

[a] *E*(1) and *E*(2) are the apparent redox potentials of the free ligands (vs Ag/AgCl) and the fully protonated or methylated ferrocene–nitrogen compounds. 8, 8*H⁺, and 8*H⁺H⁺ were reported in ref 10.

Cyclic Voltammetry

The redox potentials of the neutral ferrocene–nitrogen compounds and those of their protonated and methylated congeners are listed in Table 8. The protonated species were generated within the electrochemical cell upon treatment with a 0.54% solution of HBF_4 in CH_3CN. The methylated relatives were prepared in the reaction of $Me_3O^+BF_4^-$ with the ferrocene–nitrogen compounds. Several of the redox potentials of the neutral, protonated and methylated derivatives of **2**, **3**, **4**, and **7** have already been described in the literature;[24] however, they cannot be compared to one another as they were recorded under very different conditions.

The redox potentials of the neutral mono- and disubstituted compounds lie in a narrow range between +0.25 and +0.42 V. Upon generation of the ammonium salts the redox potentials of all compounds are shifted toward more positive values. The positive shifts caused by protonation are always smaller than in the corresponding methylated species.

Not surprisingly the different iron–nitrogen distances are reflected in different potential changes upon protonation and methylation. The smallest shift of +110 mV in **2**/**2a** is associated with the largest Fe–N distance. For **3** and **6** these distance are taken directly from the X-ray data. Due to the flexibility of the chain in the ferrocenes **2** and **7**, it is not possible to rely on X-ray

(24) *Gmelin Handbuch der Anorganischen Chemie*; Springer-Verlag: Berlin, Heidelberg, Germany, New York, 1980; Eisen-organische Verbindungen, Ferrocen A4.

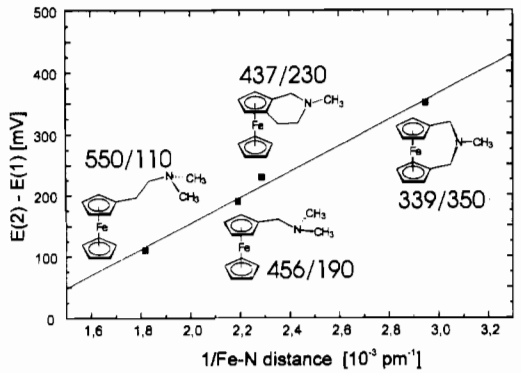

Figure 5. Plot of the inverse Fe–N distances in compounds **2**, **3**, **6** and **7** against the differences of the redox potentials of the couples **2**/**2a**, **3**/**3a**, **6**/**6a**, and **7**/**7a**.

Table 9. Comparison of the Free Enthalpies Calculated from the Iron–Nitrogen Separation and the Difference of the Redox Potentials

r, pm	ΔG_{calcd}, kcal/mol	ΔE, mV	ΔG_0, kcal/mol
339	2.72	350	8.07
437	2.17	230	5.31
456	2.03	190	4.38
550	1.68	110	2.54

data for the determination of the Fe–N distance; however, a simple molecular mechanics analysis gives a maximum value of 505 pm for **2** and 437 pm for **7**. The size of the positive shifts of the redox potentials are related to the inverse Fe–N distance and grow to a maximum value of +390 mV for a Fe–N distance of 338.5 pm in **6b**. This is illustrated for monoprotonation in the four couples **2**/**2a**, **3**/**3a**, **6**/**6a**, and **7**/**7a** in which oxidation of the ferrocene moiety reduces the basicity of nitrogen by a factor of 72, 1.3×10^3, 7.7×10^3 and 8.2×10^5. In the plot of the inverse Fe–N distances (x) vs the difference of the redox potentials (y), a linear relation is observed $y = (-2.7 + 2.1x) \times 10^2$ (Figure 5).[25] This holds true even though small changes in the geometry of the ferrocene sandwich upon oxidation are not considered in our model. It has also been shown recently by others that there is a linear relation between the size of the positive shift of the redox potential of ferrocene cryptands and the charge/radius ratio of metal cations bound within the macrocyclic cavity.[26]

In our case we have approximated the relation of the shifts in the redox potentials and the distance iron–nitrogen by a simple Coulomb point charge model.

$$W = \Delta G = \frac{z_a z_b e^2}{4\pi\epsilon_0 \epsilon r}$$

By means of this formula, two sets of values for ΔG were calculated. The first one is derived from the radius obtained from the solid state structures and the second one from the shifts of the apparent redox potentials (Table 9).

The agreement between the two values of ΔG is fairly good. This holds true even though this approach contains several obvious simplifications. It is questionable to use the bulk solvent dielectricity constant of acetonitrile for an intramolecular interaction. In addition the Coulomb model describes the interaction of point charges, which is certainly an oversimplification for the ammonium unit and the ferrocenium salt.

It is obvious that the ferrocenophane **6** has the shortest possible iron–nitrogen distance for a simple through space interaction. The only way to further increase the positive shift of the redox potential would be to directly link nitrogen to the cyclopentadienyl ring. This is evidenced in the complex 1,1′-Fc(NMe_2)$_2$, in which the redox potentials of the neutral and the methylated species differ by 1.48 V.[27] However, few ferrocenes with a direct cyclopentadienyl–nitrogen bond are known,[28] and the synthetic routes known so far are not useful for the synthesis of ferrocene crown ethers.

Lehn et al.[29] and other research groups[18,30] have investigated the very unusual proton transfer properties of cryptands. Protonation and deprotonation[31] are extremely slow reactions and lead to several isomers which are characterized by the different orientation (exo or endo) of the nitrogen lone pair with respect to the cavity of the macrocycle.[32]

To elucidate these isomerization processes, the ferrocene cryptand **8** offers the unique advantage of possessing an electrochemical probe within the macrocyclic structure. Different redox potentials caused by variable Fe–N distances in the different protonated isomers are directly accessible with cyclic voltammetry and were described recently by us.[10] At that time, we had not been able to fully explain the influence of the different isomers on the redox potentials. The results described here are sufficient to understand the protonation of **8** and to assign the structures of the different protonated isomers, which are characterized by inside and outside orientations of the N–H^+ unit with respect to the cavity of the macrocycle.[10] The similarity of the redox potentials of **4**/**4a** and **5**/**5a** with respect to the positive shifts upon protonation shows that there is no special crown effect at work. Therefore, it should be possible to compare the redox potentials of protonated ferrocene macrocycles with those of simple ferrocene amines. This assertation is further strengthened by the solid-state structure of **5a** in which it behaves like a normal diamine.

For the first protonation step of **8**, two shifts of +220 and +350 mV were recorded.[10] Not surprisingly, these values are close to the respective H^+-induced shifts of **3**/**3a** and **7**/**7a**. It is therefore quite likely that the +220-mV shift is associated with the exo-H^+ isomer and the +350-mV shift with the endo-H^+ isomer. One difficulty in the interpretation of the CV of **8** lies in the fact that it was possible to isolate neither a configurationally stable exo, exo isomer of the protonated ferrocene cryptand nor suitable crystals of a doubly protonated species.

Whereas **8** in its crystals exists exclusively as the endo, endo isomer, this is not the only isomer in solution. The analysis of the IR spectra of **8** in $CDCl_3$, following the method of Lord and Siamwiza,[33] reveals that there is a substantial amount of exo isomer. This is evidenced by an additional absorption at 2183 cm^{-1} resulting from the weak interaction of $DCCl_3$ with the nitrogen lone pair. This deuterium bridge can only form when the nitrogen lone pair is located exo with respect to the macrocyclic cavity.

However, this work has also shown that methylated ammonium salts may serve as model compounds for protonated ferrocene nitrogen compounds, as the difference of the redox shifts between related protonated and methylated species is rather small. Whereas it may not be possible to isolate a stable exo, exo protonation product of **8**, this is quite possible for the methylated species **8c**, as evidenced by the X-ray crystal structure. Under

(25) Elschenbroich, C.; Hoppe, S.; Metz, B. *Chem. Ber.* **1993**, *126*, 399.
(26) Medina, J. C.; Goodnow, T. T.; Rojas, M. T.; Atwood, J. L.; Lynn, B. C.; Kaifer, A. C.; Gokel, G. W. *J. Am. Chem. Soc.* **1992**, *114*, 10583.
(27) Stahl, K.-P.; Boche, G.; Massa, W. *J. Organomet. Chem.* **1984**, *277*, 113.
(28) (a) Bernheim, M.; Boche, G. *Angew. Chem.* **1980**, *92*, 1043; *Angew. Chem., Int. Ed. Engl.* **1980**, *19*, 1010. (b) Knox, G. R.; Pauson, P. *J. Chem. Soc.* **1961**, 4615. (c) Herberhold, M.; Ellinger, M.; Kremnitz, W. *J. Organomet. Chem.* **1983**, *241*, 227. (d) Knox, G. R.; Pauson, P. L.; Willison, D.; Solcaniova, E.; Toma, S. *Organometallics* **1990**, *9*, 301. (e) Knox, G. R.; Pauson, P. L.; Willison, D. *J. Organomet. Chem.* **1993**, *450*, 177.
(29) Smith, P. B.; Dye, J. L.; Cheney, J.; Lehn, J. M. *J. Am. Chem. Soc.* **1981**, *103*, 6044.
(30) Pizer, R. *J. Am. Chem. Soc.* **1978**, *100*, 4239.
(31) Cox, B. G.; Knop, D.; Schneider, H. *J. Am. Chem. Soc.* **1978**, *100*, 6002.
(32) Simmons, H. E.; Park, C. H. *J. Am. Chem. Soc.* **1968**, *90*, 2428.
(33) Lord, R. C.; Siamwiza, M. N. *Spectrochim. Acta* **1975**, *31A*, 1381.

the very reasonable assumption that the methylated and the protonated forms of **8** have the same overall geometry, we are now in a position to assign the redox potentials of the exo–exo and endo–endo protonated isomers in **8**. From the 40-mV difference between protonation and methylation observed in **4** and the redox potential of +0.80 V measured for **8c**, we calculate a potential of +0.76 V for endo–endo **8***H^+H^+. This value compares very well with the +0.75-V potential for the least positively shifted **8***H^+H^+ isomer.

In solution cryptand **8** exists as a mixture of exo and endo isomers. Both isomers can be protonated. Initially this gives a mixture of endo- and exo-protonated species, even though exo protonation is kinetically preferred. This mixture rearranges to finally produce the thermodynamically preferred *exo,exo*-H^+H^+ form. Methylation of **8** is only possible with the exo, exo isomer as CH_3^+ (or $O(CH_3)_3^+$) is too large to migrate into the cavity of the macrocycle. Therefore the only isomer existing in solution and the solid state is the *exo,exo*-$(CH_3)^+(CH_3)^+$ form.

Conclusions

There is a linear dependence of the positive shifts of the redox potentials in ferrocene nitrogen compounds and their protonated relatives against the inverse distance iron–nitrogen, which is in accord with a simple Coulomb model. It is also apparent that the shift of +390 mV represents the maximum value for a simple through-space interaction of the ammonium salt and the iron atom. Larger redox-switching effects will only be possible when a direct electronic interaction of the positive charge at the nitrogen with the ferrocene group is realized. Consequently future work in the area of redox-switched ferrocene crown ethers has to be directed toward directly bonding the nitrogen to the cyclopentadienyl rings.

Acknowledgment. This work was supported through the Graduiertenkolleg "Ungepaarte Elektronen in Chemie, Physik und Biologie" and through a DFG-Habiliationsstipendium to H.P. We wish to thank Prof. Dr. H. Vahrenkamp for his support and Dr. W. Deck and Dipl.-Chem. M. Ruf for the collection of the X-ray data.

Supplementary Material Available: Tables of positional parameters, thermal parameters, full bond lengths and angles, and hydrogen atom parameters in **5a**, **6c**, and **8c** (14 pages). Ordering information is given on any current masthead page.